

Preparation of Polyurethane with Zwitterionic Side Chains and Their Protein Resistance

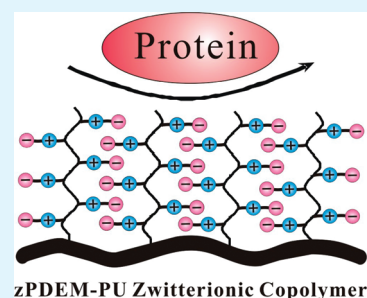
Chunfeng Ma,^{†,‡} Hao Zhou,[†] Bo Wu,[†] and Guangzhao Zhang^{*,†,‡}

[†]Hefei National Laboratory for Physical Sciences at Microscale, Department of Chemical Physics, University of Science and Technology of China, Hefei, China 230026

[‡]Faculty of Materials Science and Engineering, South China University of Technology, Guangzhou, China, 510640

ABSTRACT: Polyurethane (PU) with zwitterionic side chains has been prepared to resist nonspecific adsorption of proteins. First, dihydroxy-terminated poly(2-(dimethylamino)ethyl methacrylate) (PDEM(OH)₂) is synthesized by free radical polymerization with 3-mercapto-1,2-propanediol as the chain transfer agent, which polyadds with diisocyanate to yield a PU with PDEM side chains. Such side chains are zwitterionized by 1,3-propane sultone. Proton nuclear magnetic resonance spectroscopy (¹H NMR), Fourier transform infrared spectroscopy (FTIR), and X-ray photoelectron spectroscopy (XPS) show that the zwitterionic side chains are incorporated into the PU. Thermal analysis demonstrates the thermal stability is greatly affected by the content of the side chains. By use of quartz crystal microbalance with dissipation (QCM-D), we have investigated the adsorption of fibrinogen, bovine serum albumin, and lysozyme on a surface constructed by such a PU. It shows the PU has a controllable protein resistance depending on the content of the zwitterionic side chains.

KEYWORDS: Polyurethane, zwitterionic polymers, polyaddition, protein resistance, biofouling, QCM-D



INTRODUCTION

Nonspecific adsorption of proteins has been an important subject in a variety of biological-related processes and applications. It can induce undesirable biofouling on ship hulls, deposition of blood proteins onto medical devices, and blockage of filtration membranes in bioseparation processes.^{1–6} Poly(vinyl alcohol),⁷ heparin,⁸ polysaccharides,⁹ poly(ethylene glycol) (PEG) or oligo-(ethylene glycol),^{10–12} and zwitterionic polymers,^{13,14} have been used to inhibit or reduce protein adsorption. PEG-based materials exhibit an excellent nonfouling capability, but their long-term stability is not good enough because PEG is autoxidized relatively rapidly in the presence of oxygen and transition metal ions.¹⁵ It is recognized that protein resistance is related to the hydration of polymers.^{13,16–19} Because zwitterions such as phosphobetaine, sulfobetaine, and carboxybetaine can strongly bind water molecules via electrostatic interactions,^{13,18} they can also effectively reduce nonspecific protein adsorption. Actually, phosphobetaine with phosphorylcholine headgroups is naturally protein resistant in the outside layer of cell membranes.²⁰ Poly(sulfobetaine) and poly(carboxybetaine) with cationic and anionic groups on the same monomer residue are reported to exhibit a protein resistance similar to that of PEG-based materials.^{21–23} Yet, zwitterionic polymers are swollen in aqueous solution with low adhesion strength and low modulus, which prevents them from being used in marine antibiofouling.

Segmented polyurethane (PU) has fairly good adhesion bond and biocompatibility as well as other unique properties.^{24–26} The combination of PU and zwitterion is expected to show both

excellent protein resistance and coating ability. However, it is difficult to introduce highly polar zwitterions into the relatively hydrophobic PU chains since they are not compatible and they do not have the same solvent. So far, interpenetrating polymer networks (IPNs) of PU and zwitterionic polymers have been prepared,² and zwitterionic polymers grafted on PU surface were also reported.²⁷ However, their protein resistance and other properties are hard to manipulate.

In the present work, we have prepared dihydroxy-terminated poly(2-(dimethylamino)ethyl methacrylate) (PDEM(OH)₂) which is readily introduced into PU because of their good compatibility. The reaction of PDEM with 1,3-propane sultone yields zwitterionic side chains (zPDEM). Our aim is to provide an approach to develop materials with good protein resistance and coating ability.

EXPERIMENTAL SECTION

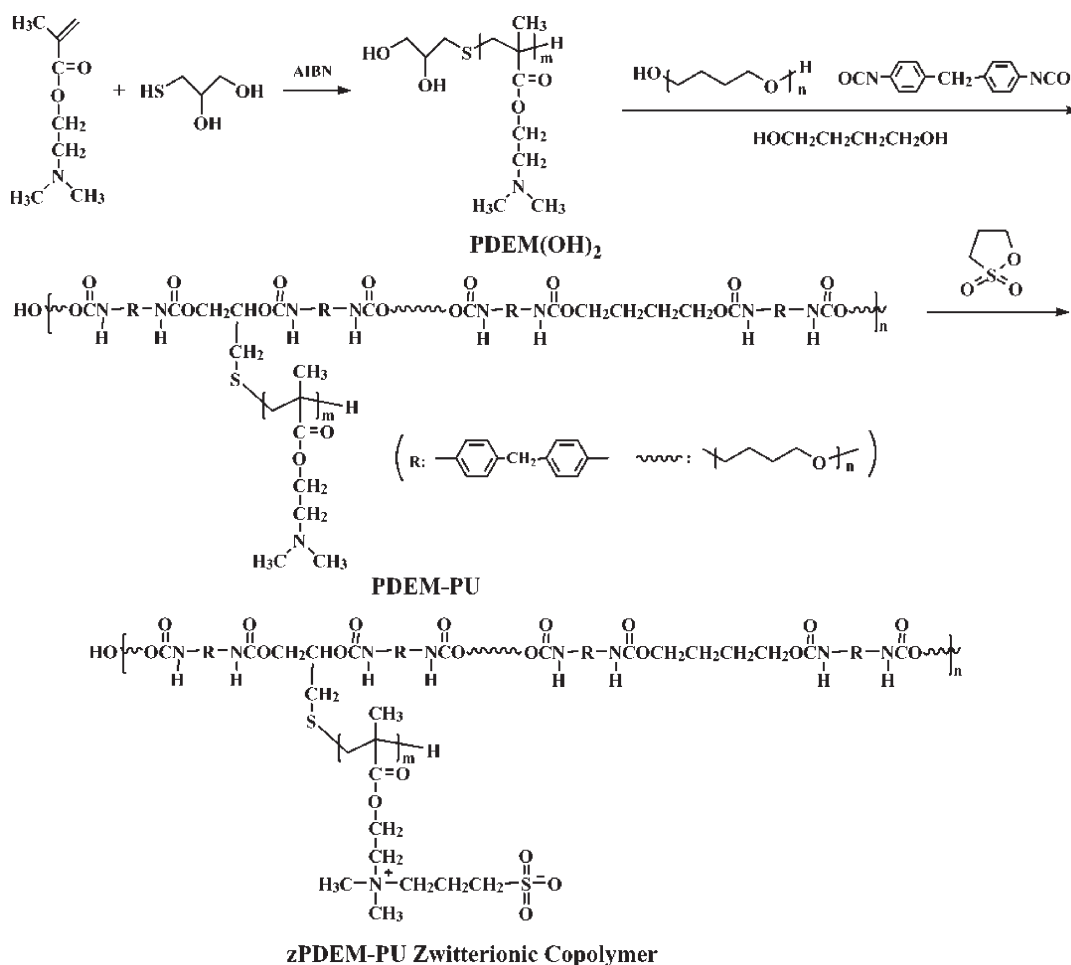
Materials. 2-(Dimethylamino)ethyl methacrylate (DEM), 1,3-propane sultone, and poly(tetramethylene oxide) (PTMG) ($M_w = 2000$ g/mol) were from Aladdin (Shanghai). 3-Mercapto-1,2-propanediol, 4,4'-diphenylmethane diisocyanate (MDI), 1,4-butane diol (1,4-BD), and dibutyltin dilaurate (DBT) were from Alfa Aesar. DEM was distilled under reduced pressure before use. 2,2-Azobisisobutyronitrile (AIBN) was used after recrystallization twice from methanol. PTMG was dried under a reduced pressure for 2 h prior to use. Tetrahydrofuran (THF) was refluxed

Received: October 27, 2010

Accepted: December 21, 2010

Published: January 11, 2011

Scheme 1. Synthesis of the Polyurethane with Zwitterionic Side Chains



over CaH_2 and distilled. Fibrinogen (fraction I from human plasma, $M_w = 340$ kDa, $pI = 5.5$) from Merck Chemicals, lysozyme via chicken egg white ($M_w = 14.7$ kDa, $pI = 11.1$) from Sangon (Shanghai), and BSA ($M_w = 68$ kDa, $pI = 4.8$) from Hualyuan Biotechnology company were used as received. Physiological phosphate buffered saline (PBS, 0.14 M, pH 7.4) was prepared by dissolving NaCl, KCl, Na_2HPO_4 , and KH_2PO_4 in Milli-Q water. Each protein solution (1.0 mg/mL) was prepared by dissolving the protein in PBS buffer. Other reagents were used as received. The synthesis of the polyurethane with zwitterionic side chains is illustrated in Scheme 1.

Synthesis of PDEM(OH)₂. PDEM(OH)₂ was prepared by radical polymerization using 3-mercapto-1,2-propanediol as chain transfer reagent to introduce a diol group at one end and control the molecular weight. In a typical experiment, DEM (3.152 g, 20 mmol), AIBN (0.0003 g, 0.01 wt % based on monomers), 3-mercapto-1,2-propanediol (0.217 g, 2 mmol), and THF (15 mL) were introduced into a Pyrex vial. After degassing by three freeze-pump-thaw cycles, polymerization was carried out at 70 °C for 12 h. The product was precipitated into hexane, filtered, and dried under vacuum. ¹H NMR (400 MHz, CDCl_3 , ppm): 4.05 ($\text{COOCH}_2\text{CH}_2$), 2.56 ($\text{CH}_2\text{N}(\text{CH}_3)_2$), 2.30 ($\text{N}(\text{CH}_3)_2$), 0.90–1.27 ($\text{CH}_2\text{C}(\text{CH}_3)\text{COO}$), 1.80–2.05 ($\text{CH}_2\text{C}(\text{CH}_3)\text{COO}$), 3.75 ($\text{HOCH}_2\text{CH}(\text{OH})$), 3.50–3.65 ($\text{HOCH}_2\text{CH}(\text{OH})$), 2.82 ($\text{CH}(\text{OH})\text{CH}_2\text{S}$). IR: 3450 cm^{-1} (OH), 2950 cm^{-1} (CH_3), 1730 cm^{-1} ($\text{C}=\text{O}$). The M_n and PDI of PDEM(OH)₂ determined by gel permeation chromatography (GPC) are 2300 g/mol and 1.47, respectively.

Synthesis of Polyurethane with PDEM side chains (PDEM-PU). PDEM-PU was synthesized via a condensation reaction in THF under a nitrogen atmosphere. MDI reacted with PTMG at 60 °C for

30 min yielding a low-molecular-weight prepolymer. After PDEM(OH)₂ was introduced, the reaction was conducted at 60 °C for another 30 min. 1,4-BD and DBT were added as the chain extender and catalyst, respectively, and the mixture was allowed to react at 70 °C for 3 h. The resulting polymers were precipitated in water and vacuum-dried for 24 h. The content of PDEM side chains was varied from 19 to 42 wt % (shown in Table 1). For comparison, PU without PDEM (PU0) was also prepared from MDI-capped PTMG and chain extender 1,4-BD. ¹H NMR (400 MHz, DMSO, ppm): 7.10 and 7.40 (C_6H_4), 3.80 ($\text{C}_6\text{H}_4\text{CH}_2$ C_6H_4), 3.30 ($\text{CH}_2\text{CH}_2\text{O}$), 1.50 ($\text{CH}_2\text{CH}_2\text{O}$), 4.10 ($\text{COOCH}_2\text{CH}_2$), 2.52 ($\text{CH}_2\text{N}(\text{CH}_3)_2$), 2.19 ($\text{N}(\text{CH}_3)_2$), 0.80–1.25 ($\text{CH}_2\text{C}(\text{CH}_3)\text{COO}$), 1.60–1.75 ($\text{CH}_2\text{C}(\text{CH}_3)\text{COO}$). IR: 3300 cm^{-1} (NH), 2950 cm^{-1} (CH_3), 2850 cm^{-1} (CH_2), 1730 cm^{-1} (COO), 1705 cm^{-1} (NHCO), 1100 cm^{-1} (C–O–C).

Betainization of PDEM-PU. PDEM-PU and 20 mol % excess of 1,3-propane sultone were dissolved in THF. The reaction was carried out at room temperature for 24 h under stirring. THF was removed by rotary evaporation, and the betainized polyurethane was redissolved in the minimum volume of deionized water. The polymer was precipitated from this aqueous solution into THF, filtered, and dried under vacuum. The degree of betainization is above 95% calculated from S/N ratio based on the DEM content in PDEM-PU from ¹H NMR.^{28,29} Table 1 summarizes the results of the PUs with varying amounts of PDEM or zPDEM and a PU without side chain as reference.

Characterization. Proton Nuclear Magnetic Resonance Spectroscopy (¹H NMR). All ¹H NMR spectra were recorded on a Bruker

Table 1. Characterization Data of PUs

sample	MDI/PTMG/PDEM(OH) ₂ / 1,4-BD ^a	side chain content (wt %)	T _i (°C) ^c	char yield (%) ^c	T _g (°C) ^d
PU0	6/1/0/5	0	250	7.2	-69
PDEM-PU19	6/1/0.4/4.6	19	229	7.7	-68, -10
PDEM-PU32	6/1/0.8/4.2	32	202	8.4	-66, -6
PDEM-PU42	6/1/1.2/3.8	42	198	9.2	-64, -2
zPDEM-PU19	^b	19	201	14.3	-67
zPDEM-PU32	^b	32	204	20.5	-65, -16
zPDEM-PU42	^b	42	206	26.6	-66, -14

^aFeed molar ratio. ^bzPDEM is synthesized by the reaction of PDEM with 1,3-PS (20 mol % excess based on DEM). ^cDetermined by TGA.

^dDetermined by DSC.

AV400 NMR spectrometer using CDCl₃ or DMSO as solvent and tetramethylsilane (TMS) as internal standard.

Fourier Transform Infrared Spectroscopy (FTIR). FTIR spectra were recorded on a Bruker VECTOR-22 IR spectrometer. The spectra were collected at 64 scans with a spectral resolution of 4 cm⁻¹ by the KBr disk method.

Gel Permeation Chromatography (GPC). The number and weight-average molecular weights (*M_n* and *M_w*) and molecular weight distribution (*M_w*/*M_n*) were determined by GPC at 35 °C on a Waters 1515 using a series of monodisperse polystyrenes as standard and THF as the fluent with a flow rate of 1.0 mL/min.

X-ray Photoelectron Spectroscopy (XPS). XPS measurements were performed on an X-ray photoelectron spectrometer (ESCALAB 250, Thermo-VG Scientific Corporation) with a monochromatic focused Al Kα X-ray source (1486.6 eV). All core-level spectra were referenced to the monochromatic Mg X-ray source (1253.6 eV). The detection was performed at 45° with respect to the sample surfaces. The pressure in the sample chamber was maintained at 10⁻⁹ mbar. All spectra were charge corrected for the C1s peak at 284.7 eV.

Thermal Analysis. Thermogravimetric analysis (TGA) was performed on a TA SDT Q600 instrument under nitrogen atmosphere at a heating rate of 10 °C/min in the range 25 to 800 °C. Differential scanning calorimetry (DSC) was performed on a TA Instruments Q2000 differential scanning calorimeter under a nitrogen flow of 50 mL/min. Samples were quickly heated to 120 °C and kept for 5 min to remove thermal history, then cooled to -90 °C at a rate of 10 °C/min, and finally were reheated to 120 °C at the same rate. All DSC traces are from the second heat to minimize effects of thermal history. Glass transition temperatures (*T_g*) were taken as the midpoint of the transition.

QCM-D Measurements. QCM-D and the AT-cut quartz crystal with a fundamental resonant frequency of 5 MHz were from Q-sense AB.³⁰ The quartz crystal was mounted in a fluid cell with one side exposed to the solution. The effects of surface roughness were minimized by using highly polished crystals with a root-mean-square roughness less than 3 nm.³¹ The details about the QCM-D can be found elsewhere.³⁰⁻³³ Briefly, the mass of a thin layer on quartz crystal relates to the decrease in the resonant frequency of the crystal, whereas the dissipation factor is related to the viscoelastic properties of the additional layer. In the present study, the changes in the frequency (Δf) and dissipation (ΔD) give the information about the protein adsorption and structural change of the protein layer. All the presented data are from the third overtone (*n* = 3). Δf and ΔD values from the fundamental were discarded because they were usually noise due to insufficient energy trapping.³⁴ Data from the fifth and seventh overtones were not presented since they were similar to those from the third overtone. The experiments were performed at 25 °C with PBS as the reference.

RESULTS AND DISCUSSION

Figure 1 shows the typical ¹H NMR spectrum obtained from DEM, PDEM(OH)₂ and PDEM-PU32. The absence of double

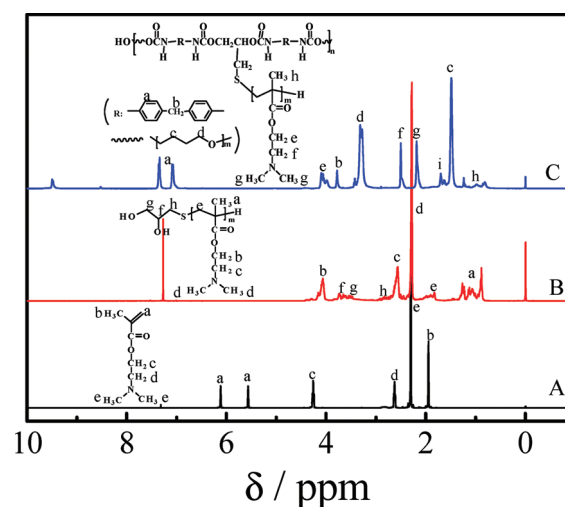


Figure 1. ¹H NMR spectra of (A) DEM in CDCl₃, (B) PDEM(OH)₂ in CDCl₃, and (C) PDEM-PU32 in DMSO-*d*₆.

bonds ($\delta = 5.60$ and $\delta = 6.20$) and sulfhydryl group ($\delta = 1.77$) indicates that DEM telomerize into PDEM(OH)₂. All the peaks from PDEM and PU were presented except the signals of methine ($\delta = 3.75$) and methylene ($\delta = 3.50$ – 3.65) in PDEM(OH)₂, indicating that all the terminal hydroxyl groups completely converted and the PDEM(OH)₂ is incorporated into the PU. zPDEM-PU32 was not measured by ¹H NMR since no deuterated solvent is available for it.

Figure 2 shows the typical FTIR spectra of DEM, PDEM(OH)₂, PDEM-PU32, and zPDEM-PU32. The absence of double bonds (1640 cm⁻¹) and the presence of hydroxyl (3450 cm⁻¹) further indicate the structure of PDEM(OH)₂. For PDEM-PU32, the peaks at 3307 cm⁻¹ corresponding to the urethane amide bond and the absence of peaks for hydroxyls in PDEM(OH)₂ indicate the incorporation of PDEM. As regards zPDEM-PU32, the presence of the absorbance at 1036 cm⁻¹ (the stretching vibrations of -SO₃ groups) indicates the betainization of PDEM-PU. In contrast to PDEM-PU32, zPDEM-PU32 has a broader urethane amide band, and the intensity of free NH stretching (3450 cm⁻¹) increases. This is because the betainization can destroy the dipole-dipole interactions between the dimethylamino groups in side chains and NHCOO groups in the main chains, and the phase separation between them increases.³⁶

Figure 3A shows the XPS spectra corresponding to N_{1s}. The peak at 400 eV is attributed to nitrogen atom in the PU or PDEM. Theoretical contents of N element in PU0 and PDEM-PU32 are 4.25 and 5.79 wt %, respectively, and the corresponding

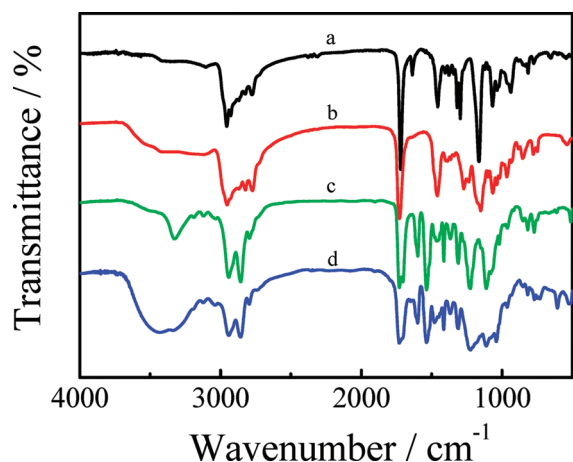


Figure 2. FTIR spectra of (a) DEM, (b) PDEM(OH)₂, (c) PDEM-PU32, and (d) zPDEM-PU32.

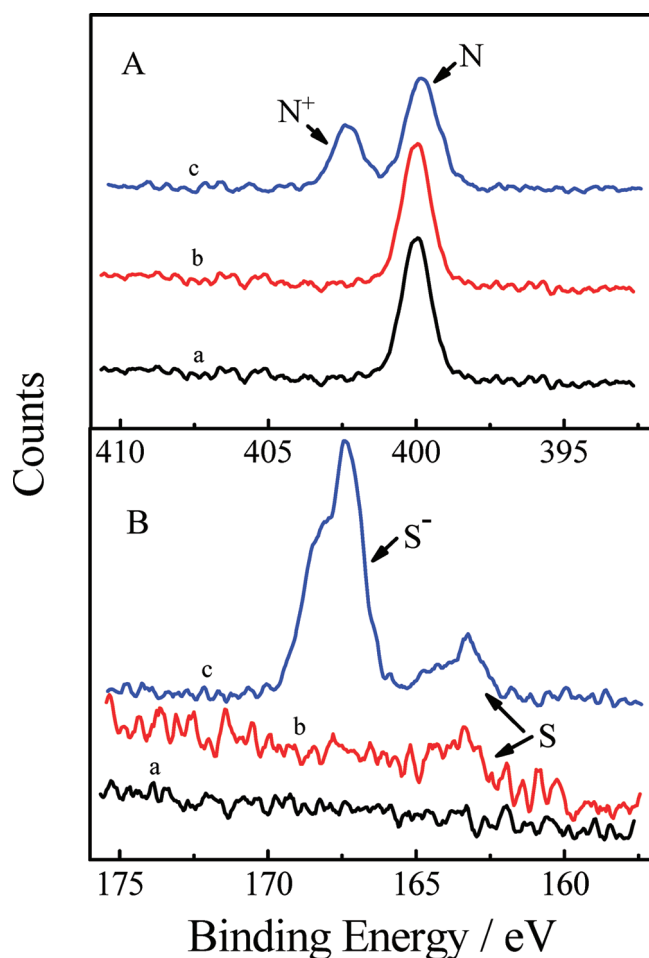


Figure 3. (A) XPS spectra corresponding to the N_{1s} of (a) PU0, (b) PDEM-PU32, and (c) zPDEM-PU32. (B) XPS spectra corresponding to the S_{2p} of (a) PU0, (b) PDEM-PU32, and (c) zPDEM-PU32.

experimental values are 3.31 and 3.85 wt %. Considering that XPS measures the elements on surface, it is understandable that the experimental values are lower than theoretical values since only part of N element is distributed on the PU surface. On the other hand, the fact that the N content in PDEM-PU32 increases in comparison

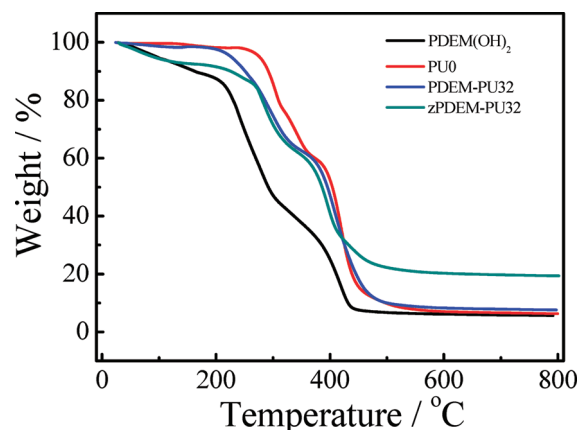


Figure 4. TGA curves of PDEM(OH)₂, PU0, PDEM-PU32, and zPDEM-PU32.

with that in PU0 clearly indicates that PDEM is incorporated into PU. For zPDEM-PU32, the peaks at 400 and 402.5 eV were attributed to the nitrogen in PDEM and that in sulfobetaine group, respectively. Figure 3B shows the XPS spectra corresponding to S_{2p}. A new peak at 163 eV in PDEM-PU32 can be observed in comparison with PU0, which was attributed to the sulfur atoms from telomerization of DEM using 3-mercapto-1,2-propanediol as chain transfer reagent. For zPDEM-PU32, like the case in PDEM-PU32, the peak at 163 eV is attributed to the sulfur atoms, whereas the peak at 167 eV is attributed to the sulfur atom in sulfonate (−SO₃) groups. The facts further demonstrate that the zwitterionic chains are introduced to the polyurethane.

Figure 4 shows the TGA thermograms of PDEM(OH)₂, PDEM-PU32, zPDEM-PU32, and PU0. PDEM(OH)₂ shows an initial weight loss below 100 °C. This is probably due to the loss of the water absorbed in the sample. A prominent decomposition can be observed at ~200 °C, indicating the limited thermal stability of PDEM. The decomposition of PU0 consists of a small drop below 270 °C and a main loss weight at approximately 380 °C. The former is associated with the decomposition of the urethane bonds while the latter is associated with the soft segment scission. PDEM-PU32 is decomposed at 230 °C, lower than that of PU0, indicating that the presence of PDEM side chains can decrease the thermal stability. For zPDEM-PU32, the initial decomposition temperature is close to that of PDEM-PU32, indicating that the betainization of PDEM has a slight effect on the thermal stability. However, the overall final char yield increases up to 20% due to the increase of S element.¹⁷ This also suggests that the zwitterionic chains have been introduced to the polyurethane.

Figure 5 shows the DSC thermogram for PDEM(OH)₂, PDEM-PU32, zPDEM-PU32, and PU0. The temperatures about the thermal transition are listed in Table 1. PDEM(OH)₂ exhibits a T_g at −12 °C without melting or crystallization. PU0 has a T_g around −69 °C, and a melting peak at 14 °C due to the melting of crystallized PTMG segments.³⁵ PDEM-PU32 exhibits two T_g at −66 °C and −6 °C, which arise from the PU segments and PDEM, respectively. Note that the latter (−6 °C) is higher than the corresponding T_g (−12 °C) of PDEM(OH)₂. This is because the dipole–dipole interactions between the dimethyl-amino groups and NHCOO groups increase the compatibility between PDEM and PU blocks.³⁶ In addition, PDEM-PU32 exhibits a melting peak much smaller than that in PU0. This is also due to the interactions between PDEM and PU, which can restrict the mobility of polymer chain and reduce the crystallinity

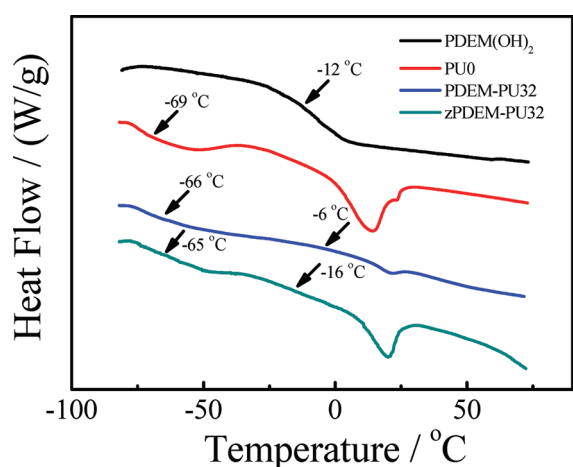


Figure 5. DSC curves of PDEM(OH)₂, PU0, PDEM-PU32, and zPDEM-PU32.

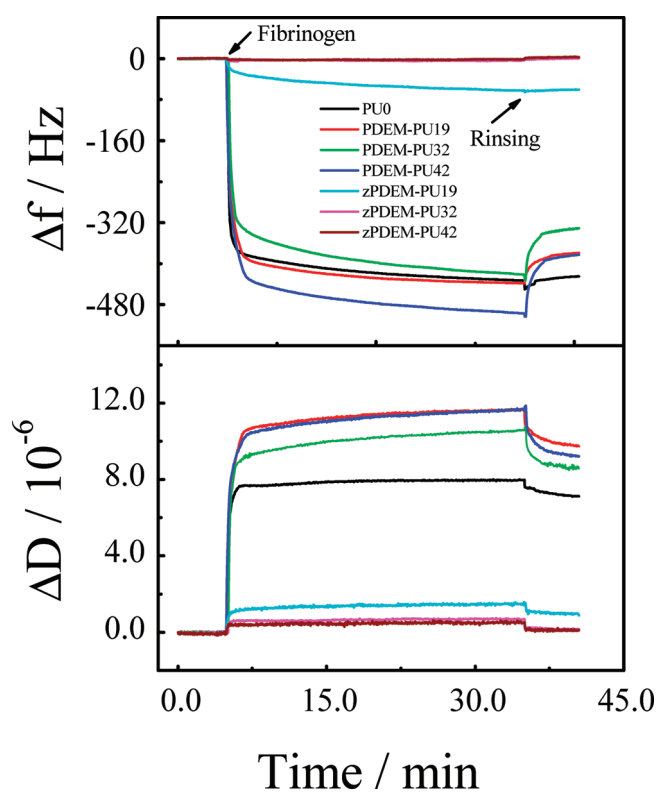


Figure 6. Time dependence of frequency shift (Δf) and dissipation shift (ΔD) for the adsorption of fibrinogen on a polymeric surface at 25 °C.

of PTMG segment.^{36,37} zPDEM-PU32 also exhibits two T_g at -65 °C and -16 °C. Obviously, the latter (-16 °C) is lower than the corresponding T_g (-6 °C) of PDEM-PU32 because the zwitterionization can weaken the dipole–dipole interactions between the dimethylamino groups in side chains and NHCOO groups in the main chains, and the phase separation between them increases. As a result, the T_g shifts to that of PDEM(OH)₂ homopolymer. For the same reason, PTMG segments are much less geometrically constrained,³⁷ and a more obvious melting peak is observed in zPDEM-PU32.

We have examined the protein resistance of the PUs by use of QCM-D. Figure 6 shows the time dependence of frequency shift

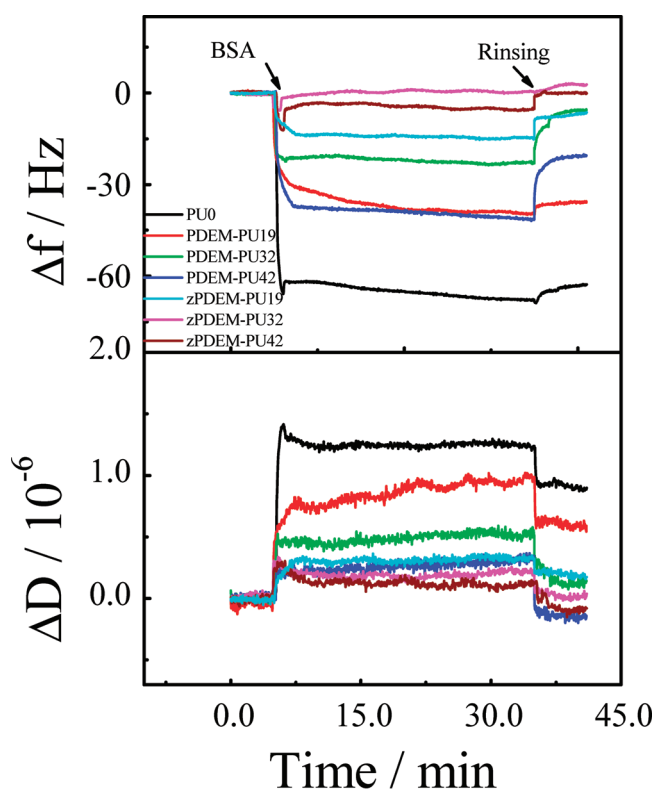


Figure 7. Time dependence of frequency shift (Δf) and dissipation shift (ΔD) for the adsorption of BSA on a polymeric surface at 25 °C.

(Δf) and energy dissipation shift (ΔD) for adsorption of fibrinogen on different PU surfaces. For PU0 and PDEM-PUs with different PDEM loadings, after fibrinogen is introduced, Δf sharply decreases and then gradually levels off. Upon rinsing with PBS, Δf exhibits a marked decrease in comparison with the baseline for PBS. It is known that the increase in mass on the sensor surface causes the frequency to decrease. The decrease in Δf indicates the adsorption of fibrinogen on the surfaces. On the other hand, it is known that ΔD increases with the thickness but decreases with the rigidity of a layer. The marked increase in ΔD relative to the baseline further indicates that fibrinogen is adsorbed forming a viscoelastic layer. Fibrinogen is a large blood plasma protein that can strongly adsorb onto hydrophobic surfaces. Moreover, PDEM is a weak polyelectrolyte, which is positively charged under the experiment condition (PBS, 0.14 M, pH 7.4). The adsorption was likely electrostatically driven. For zPDEM-PUs, even when zPDEM content is 19 wt % (zPDEM-PU19), Δf and ΔD changes are less than those in the case of PU0 or PDEM-PUs with different PDEM loadings. When zPDEM content is above 32 wt % (zPDEM-PU32 or zPDEM-PU42), Δf and ΔD return to the baselines after the rinsing with PBS, indicating no fibrinogen is adsorbed. Accordingly, the protein resistance of the materials depends on the zPDEM content.

Figure 7 shows the time dependence of frequency shift (Δf) and energy dissipation shift (ΔD) for adsorption of BSA on different PU surfaces. BSA with a smaller size than fibrinogen is the most abundant protein in blood. For PU0, Δf decreases and ΔD increases markedly, indicating the adsorption of BSA on the surface. For PDEM-PUs, the decrease in Δf and increase in ΔD become smaller in comparison with those in the case of PU0, indicating that the BSA adsorption on PDEM-PU becomes less. Similar to fibrinogen adsorption onto the zPDEM-PUs, either Δf or ΔD

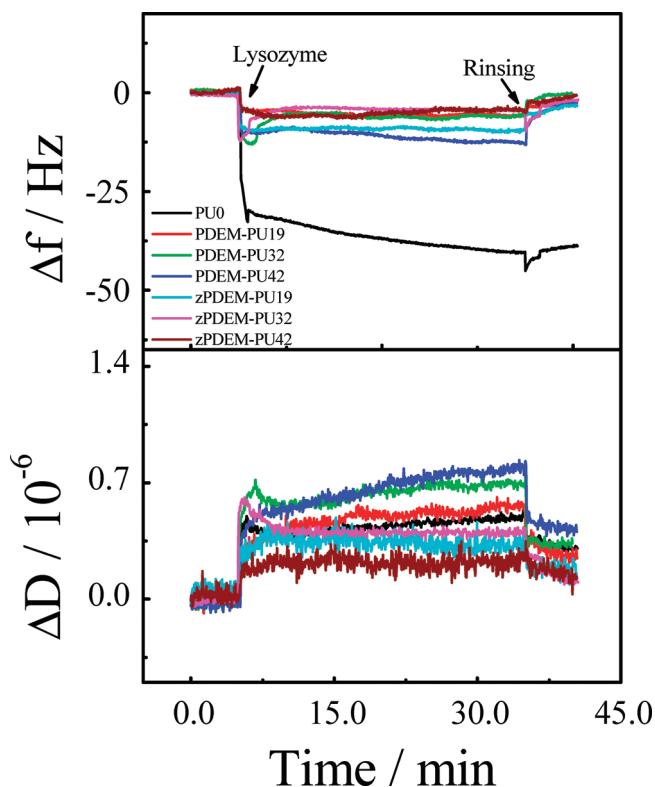


Figure 8. Time dependence of frequency shift (Δf) and dissipation shift (ΔD) for the adsorption of lysozyme on a polymeric surface at 25 °C.

slightly changes after BSA solution is introduced. Clearly, when zPDEM content is above 19 wt %, the zPDEM-PU can resist the BSA adsorption.

Figure 8 shows the time dependence of frequency shift (Δf) and energy dissipation shift (ΔD) for the adsorption of lysozyme on different PU surfaces. Lysozyme is the smallest in size among the three proteins studied, which is positively charged under the condition (PBS, 0.14 M, pH 7.4). For hydrophobic PU0, the marked decrease in Δf and increase in ΔD indicate the adsorption of lysozyme on the surface. For either PDEM-PU or zPDEM-PU, lysozyme is slightly adsorbed, reflecting in the small changes in Δf and ΔD before and after lysozyme solution is introduced. Thus, the PDEM-PU can resist lysozyme adsorption at pH 7.4 due to the electrostatic repulsion between the positively charged lysozyme and PDEM.

The above studies show PUs with zwitterionic side chains can resist the nonspecific adsorption of proteins with different sizes and charging levels when the zwitterion concentration is high enough. It is reported that PUs with surface-grafted zwitterionic groups also show good protein resistance, where PU serves as a substrate and the protein resistance depends on the grafting density and thickness of zwitterionic polymer.^{27,38} Clearly, such surface-grafting is not applicable to a large-scale antibiofouling. IPNs of segmented PU and SBMA have protein resistance depending on the content and distribution of SBMA units.² However, the protein resistance is hard to control since the distribution of SBMA monomers depends on their diffusion in the PU network. The approach presented in this study can readily incorporate zwitterionic side chains into polyurethane, which combines the protein resistance of zwitterionic polymers and unique properties of polyurethanes. Furthermore, the properties of the materials can be tuned by varying the content of zwitterions.

CONCLUSION

In conclusion, we have prepared polyurethanes with zwitterionic side chains by combination of free radical polymerization and polyaddition. The polyurethanes were characterized by ¹H NMR, FTIR, and XPS. Thermal analysis studies demonstrated that the incorporation of zwitterionic side chains can decrease the thermal stability of the polyurethane. QCM-D studies showed that the polyurethane can effectively resist nonspecific protein adsorption when the content of zwitterionic side chains is high enough.

AUTHOR INFORMATION

Corresponding Author

*E-mail: gzzhang@ustc.edu.cn.

ACKNOWLEDGMENT

The financial support of the National Distinguished Young Investigator Fund (20725414), the Science and Technology Cooperation Project of China and Australia (51011120051), and Ministry of Science and Technology of China (2007CB936401) is acknowledged.

REFERENCES

- (1) Kane, R. S.; Deschatelets, P.; Whitesides, G. M. *Langmuir* **2003**, *19*, 2388.
- (2) Chang, Y.; Chen, S. F.; Yu, Q. M.; Zhang, Z.; Bernards, M.; Jiang, S. Y. *Biomacromolecules* **2007**, *8*, 122.
- (3) Senaratne, W.; Andruzzi, L.; Ober, C. K. *Biomacromolecules* **2005**, *6*, 2427.
- (4) Metzke, M.; Bai, J. Z.; Guan, Z. B. *J. Am. Chem. Soc.* **2003**, *125*, 7760.
- (5) Schön, P.; Görlich, M.; Coenen, M. J. J.; Heus, H. A.; Speller, S. *Langmuir* **2007**, *23*, 9921.
- (6) Williams, D. F. *Biomaterials* **2008**, *29*, 2941–2953.
- (7) Amanda, A.; Mallapragada, S. K. *Biotechnol. Prog.* **2001**, *17*, 917.
- (8) Johnell, M.; Larsson, R.; Siegbahn, A. *Biomaterials* **2005**, *26*, 1731.
- (9) McArthur, S. L.; Mclean, K. M.; Kingshott, P.; St John, H. A. W.; Chatelier, R. C.; Griesser, H. J. *Colloids Surf., B* **2000**, *17*, 37.
- (10) Prime, K. L.; Whitesides, G. M. *J. Am. Chem. Soc.* **1993**, *115*, 10714.
- (11) Roberts, C.; Chen, C. S.; Mrksich, M.; Martichonok, V.; Ingber, D. E.; Whitesides, G. M. *J. Am. Chem. Soc.* **1998**, *120*, 6548.
- (12) Harris, J. M. *Poly(ethylene glycol) Chemistry: Biotechnical and Biomedical Applications*; Plenum Press: New York, 1992.
- (13) Chen, S. F.; Zheng, J.; Li, L. Y.; Jiang, S. Y. *J. Am. Chem. Soc.* **2005**, *127*, 14473.
- (14) Holmlin, R. E.; Chen, X. X.; Chapman, R. G.; Takayama, S.; Whitesides, G. M. *Langmuir* **2001**, *17*, 2841.
- (15) Lewis, A. L. *Colloids Surf., B* **2000**, *18*, 261.
- (16) Jiang, S. Y.; Cao, Z. Q. *Adv. Mater.* **2010**, *22*, 920.
- (17) Liu, P. S.; Chen, Q.; Liu, X.; Yuan, B.; Wu, S. S.; Shen, J.; Lin, S. C. *Biomacromolecules* **2009**, *10*, 2809.
- (18) He, Y.; Hower, J.; Chen, S. F.; Bernards, M. T.; Chang, Y.; Jiang, S. Y. *Langmuir* **2008**, *24*, 10358.
- (19) Ma, C. F.; Hou, Y.; Liu, S.; Zhang, G. Z. *Langmuir* **2009**, *25*, 9467.
- (20) Nakabayashi, N.; Williams, D. F. *Biomaterials* **2003**, *24*, 2431.
- (21) Zhang, Z.; Chao, T.; Chen, S. F.; Jiang, S. Y. *Langmuir* **2006**, *22*, 10072.
- (22) Chang, Y.; Chen, S. F.; Zhang, Z.; Jiang, S. Y. *Langmuir* **2006**, *22*, 2222.
- (23) Zhang, Z.; Chen, S. F.; Chang, Y.; Jiang, S. Y. *J. Phys. Chem. B* **2006**, *110*, 10799.
- (24) Tan, H.; Liu, J.; Li, J. H.; Jiang, X.; Xie, X. Y.; Zhong, Y. P.; Fu, Q. *Biomacromolecules* **2006**, *7*, 2591.

- (25) Lim, H.; Lee, Y.; Park, I. J.; Lee, S. B. *J. Colloid Interface Sci.* **2001**, *241*, 269.
- (26) Fournier, D.; Prez, F. D. *Macromolecules* **2008**, *41*, 4622.
- (27) Zhang, J.; Yuan, Y. L.; Wu, K. H.; Shen, J.; Lin, S. C. *Colloids Surf., B* **2003**, *28*, 1.
- (28) Lascelles, S. F.; Malet, F.; Mayada, R.; Billingham, N. C.; Armes, S. P. *Macromolecules* **1999**, *32*, 2462.
- (29) Butun, V.; Bennett, C. E.; Vamvakaki, M.; Lowe, A. B.; Billingham, N. C.; Armes, S. P. *J. Mater. Chem.* **1999**, *7*, 1693.
- (30) Rodahl, M.; Höök, F.; Krozer, A.; Kasemo, B.; Breszinsky, P. *Rev. Sci. Instrum.* **1995**, *66*, 3924.
- (31) Daikhin, L.; Urbakh, M. *Faraday Discuss.* **1997**, *107*, 27.
- (32) Sauerbrey, G. *Z. Phys.* **1959**, *155*, 206.
- (33) Voinova, M. V.; Rodahl, M.; Jonson, M.; Kasemo, B. *Phys. Scrip.* **1999**, *59*, 391.
- (34) Bottom, V. E. *Introduction to Quartz Crystal Unit Design*; Van Nostrand Reinhold Co.: New York, 1982.
- (35) Hu, C. B.; Ward, R. S.; Schenider, N. S. *J. Appl. Polym. Sci.* **1982**, *27*, 2167.
- (36) Nayak, S.; Verma, H.; Kannan, T. *Colloid Polym. Sci.* **2010**, *288*, 181.
- (37) Williams, S. R.; Wang, W. Q.; Winey, K. I.; Long, T. E. *Macromolecules* **2008**, *41*, 9072.
- (38) Li, Y. J.; Hanada, T.; Nakaya, T. *Chem. Mater.* **1999**, *11*, 763.